

Polymeric Systems for Acoustic Damping. I. Poly(vinyl Chloride)-Segmented Polyether Ester Blends

D. J. HOURSTON and I. D. HUGHES, *Department of Chemistry,
University of Lancaster, Bailrigg, Lancaster LA1 4YA, U.K.*

Synopsis

A series of six Hytrel/PVC blends were prepared by solution blending Hytrel in methylene chloride and PVC in tetrahydrofuran. The samples were subsequently prepared in sheet form by hot pressing at 170°C. Physical and mechanical properties of the homopolymers and the blends were investigated. The copolyester homopolymer is a partly crystalline elastomeric material. The level of crystallinity was measured by x-ray diffraction and the sensitivity of this level to heat treatments and quenching determined by DSC. A Morgan pulse propagation meter was used to measure sonic velocity and, indirectly, acoustic impedance of the blends. Dynamic mechanical studies indicated that blends containing 25%–50% by weight of Hytrel were completely compatible in the sense that a single glass transition was observed; but as the Hytrel level was increased to 60% and 65%, a shoulder became apparent on the low-temperature side of the glass transition peak. At 80% Hytrel, two peaks were observed, indicating incompatibility. The glass transition temperatures of these blends were found to decrease linearly with added Hytrel.

INTRODUCTION

This paper is the first of a series of reports on investigations into the use of a variety of polymeric systems as possible acoustic damping materials. The increased awareness of noise as a health hazard is leading to the search for more effective noise attenuation systems. A considerable amount of noise originates in machinery because of the inherently very low damping character of metals. The physical properties of a material which influences its sound insulation performance are stiffness, surface mass, and damping characteristics.¹

As far as polymers are concerned, it is likely that systems having high damping will not have particularly high moduli. If stiffness becomes an important factor in any given sound insulation application, it is possible to use constrained layer damping^{2,3} where the polymeric damping material is trapped between stiff outer skins such as metal sheet. The surface mass of polymeric damping materials may be enhanced by the incorporation of dense fillers such as barytes or lead, but this will result in a reduction in the maximum level of damping.

This and future work will be concerned primarily with the search for materials exhibiting high damping in the appropriate frequency/temperature range. The acoustic spectrum is generally regarded as extending from 20 Hz to 20 kHz, so it is necessary to have as large and as broad a relaxation dispersion over as much of this frequency range as possible.

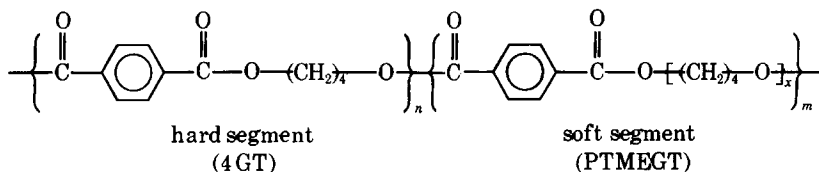
The most commonly used damping materials in acoustic and mechanical energy absorption are homopolymers and copolymers^{4,5} having a glass transition in the appropriate region. Such damping peaks are generally rather narrow, covering a temperature range of about 30°C for a given frequency in the acoustic range. Polymer blends of varying degrees of compatibility have also been investigated^{6,7} and generally lead to a broader loss mechanism than is the case for homopolymers and copolymers alone. Recent work by Sperling and co-workers^{8,9} into loss mechanism broadening in interpenetrating polymer network systems has resulted in interesting acoustic damping materials.

In this paper, we are largely concerned with compatible blends of poly(vinyl chloride) (PVC) and a relatively new commercial (du Pont) segmented polyether ester copolymer.¹⁰⁻¹³ Nishi, Kwei, and Wang¹⁴ and Kwei and Nishi¹⁵ have reported on certain mechanical properties of this system including the influence of heat treatments.

EXPERIMENTAL

Polymers

HytreI. This segmented polyether ester (grade 4055) was kindly supplied by the E. I. du Pont de Nemours Company and had been prepared by melt transesterification of dimethyl terephthalate, poly(tetramethylene ether) glycol, and 1,4-butanediol. The product is a random block copolymer of crystallizable tetramethylene terephthalate (4GT), which forms the hard segments, and poly(tetramethylene ether) glycol terephthalate, which forms the soft segments. The structural formula is shown below:



Poly(vinyl Chloride). A rigid poly(vinyl chloride), Corvic (D60/11), containing no plasticizer was used.

The characterization data for both polymers are shown in Table I.

Preparation of Samples

Six HytreI/PVC blends were prepared by solution blending where the HytreI in methylene chloride and the PVC in tetrahydrofuran were mixed and the

TABLE I
Characterization Data for the Poly(vinyl Chloride) and HytreI Samples
Used in the Preparation of the Blends

	Poly(vinyl chloride)	HytreI
$\bar{M}_n \times 10^{-3}$	80	30
\bar{M}_w/\bar{M}_n^a	—	1.56
Density, g/cm ^{3b}	1.415	1.152

^a By GPC.

^b 23°C.

polymer precipitated by the addition of an excess of methanol. The precipitated blend was centrifuged and then vacuum dried at ambient temperature for two to three days prior to sheeting in a hot press (170°C). These mechanically isotropic sheets had a thickness of 0.5 ± 0.05 mm. The composition of the blends formed were 25:75, 45:55, 50:50, 60:40, 65:35, and 80:20 Hytrel to PVC, respectively.

Measurements

The number-average molecular weights of the homopolymers were measured using a Model 501 Mecrolab membrane osmometer. The Hytrel sample was measured in chloroform and the PVC sample, in tetrahydrofuran. Density measurements were made in a Davenport density gradient column apparatus at 23°C using a carbon tetrachloride-xylene system. The molecular weight distribution of the Hytrel sample was investigated using a Waters GPC apparatus (Model 502).

Crystallinity measurements were made by the wide-angle x-ray diffraction technique using $\text{Cu}(\text{K}\alpha)$ radiation. The angular (2θ) range covered was from 7° to 31° with 30-sec intensity readings automatically recorded every 6 min of angle. A Perkin-Elmer differential scanning calorimeter (Model DSC-2) was used at a heating rate of 10°C/min to study the transitions in the Hytrel sample and the effect of thermal treatments on this material.

The reported longitudinal sonic velocity measurements utilized a Morgan pulse propagation meter (Model PPM-5R) which measures the time elapsed in microseconds between the transmission and the subsequent reception of a sound pulse through a known distance in the sheet sample. The dynamic mechanical experiments were conducted using a Rheovibron dynamic viscoelastometer (Model DDV-II). The error involved in determining the glass transition temperature from these data was estimated to be $\pm 1.5^\circ\text{C}$.

RESULTS AND DISCUSSION

Crystallinity and Thermal Treatments

A number of papers^{10,11,13} have described morphological studies of the segmented polyether ester Hytrel. This polymer has been shown to be semicrystalline under certain conditions showing a spherulitic texture with the hard segments (4GT) forming the crystalline phase. Electron microscopy indicates¹⁰ that Hytrel has a two-phase structure consisting of continuous and interpenetrating amorphous and crystalline domains.

In addition to the characterization data shown in Table I, proton NMR was used to estimate the average hard-segment block length. This sample was found to contain 84 mole-% of hard segments having, on average, six 4GT repeat units per block.

Wide-angle x-ray diffraction of the as-received Hytrel lead to scattering intensity-versus-scattering angle (2θ) plots with two peaks (21.5° and 23.5°) and a shoulder at 16.5°. Figure 1 shows a schematic diagram of scattering intensity versus scattering angle from Hytrel. The lower amorphous curve was obtained from a sample held at 200°C for approximately 5 min and then quickly plunged

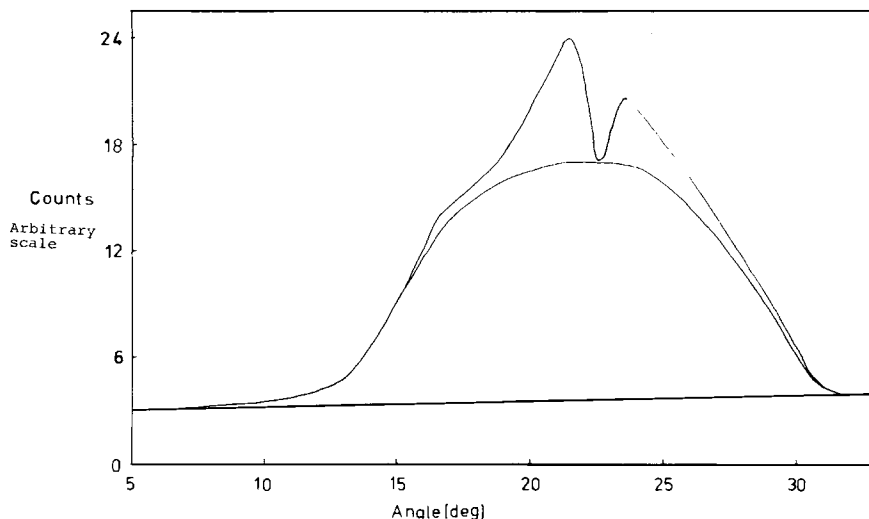


Fig. 1. Scattering intensity vs scattering angle (2θ) diagram for the original Hytrel sample.

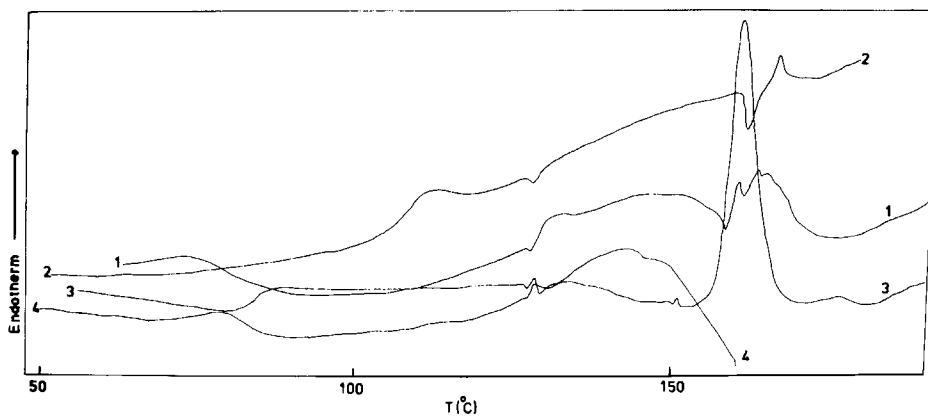


Fig. 2. DSC thermograms of the original and heat-treated Hytrel samples. Curve 1: as received; curve 2: annealed at 100°C for 2 hr; curve 3: annealed at 150°C for 2 hr; curve 4. Sample quenched from 180°C .

into liquid nitrogen and stored there until required. The degree of crystallinity calculated by area measurement was found to be 20%.

Figure 2 shows DSC thermograms of the original Hytrel sample (curve 1), a sample annealed at 100°C for 2 hr (curve 2), a sample annealed at 150°C for 2 hr (curve 3), and a sample which has been heated to 180°C and then quenched in liquid nitrogen (curve 4). Curve 3 shows a hard-segment glass transition at about 80°C , which is in good agreement with a literature value¹⁶ for the 4GT homopolyester. Above this temperature in the as-received sample (curve 1), there is a crystallization exotherm which is absent in curve 2 when the sample had been heated at 100°C for 2 hr prior to the DSC experiment. In the case of curve 3, it is clear that annealing at 150°C for 2 hr results in more or less complete crystallization as there is, again, no evidence of crystallization during the actual DSC experiment. The absence of a hard-segment glass transition in curve 2,

but not in curve 3, is thought to be the result of the development of spherulitic structures with interfibrillar amorphous regions at the higher annealing temperature. In the sample annealed at only about 20°C above the hard-segment glass transition temperature, the crystallites are thought to be small but to involve virtually all the hard-segment blocks. There is a small endotherm centered at about 112°C which is thought to be the result of the melting of these small and imperfect crystalline structures. The inflection points in all four thermograms at about 128°C are the result of an instrumental abnormality.

Curves 1 and 2 show a broad endotherm covering the 100°–170°C range which is ascribed to the melting of hard-segment crystalline structures having a wide variety of imperfections. Annealing at 100°C for 2 hr did not appreciably alter the overall level of crystallinity nor did it significantly narrow the melting range. However, annealing at 50°C higher led to a fairly sharp melting point at 162°C. The quenched sample (curve 4) also showed an endotherm, but at a somewhat lower temperature than for the other three curves. It is clear that this sample is also crystallizing during the DSC experiment. In the x-ray diffraction experiments, it was difficult to achieve an amorphous sample and it was necessary to store the sample at low temperature until it was required.

The melting point of the annealed sample (curve 3) was in poor agreement with the reported values of 150°C by Nishi et al.¹⁴ and 185°C by Shen et al.¹³ and also differs substantially from the literature value¹⁷ of 232°C for the 4GT homopolymer. The Hytrel samples showed evidence of considerable degradation prior to reaching this temperature.

The thermograms for the blends were very similar to both curve 1 in Figure 2 and to the data published by Nishi et al.¹⁴ for a 50:50 blend.

Sonic Velocity and Dynamic Mechanical Measurements

Table II and Figure 3 present the sonic pulse propagation data for both the homopolymers and for the six blends. The longitudinal sonic velocity (V_L) increases essentially linearly with the weight percent of PVC in the blend up to around 50%. There is then a more rapid increase in V_L with increasing PVC content. It is thought that this increase in slope occurs when PVC becomes a continuous phase. The sample containing 20% by weight of PVC displayed two

TABLE II
Longitudinal Sonic Velocity (V_L) and Acoustic Impedance (Z) Data for
Homopolymers and Blends at 20°C^a

Composition ^b	V_L , km/sec	$Z \times 10^{-6}$, g/cm ² ·sec
100	0.28	0.03
80	0.51	0.06
65	0.68	0.08
60	0.81	0.10
50	0.96	0.12
45	0.92	0.12
25	1.77	0.24
0	1.83	0.26

^a $Z = \rho \cdot V_L$, where ρ is the density of the polymeric sheet.

^b Weight percent of Hytrel in the blends.

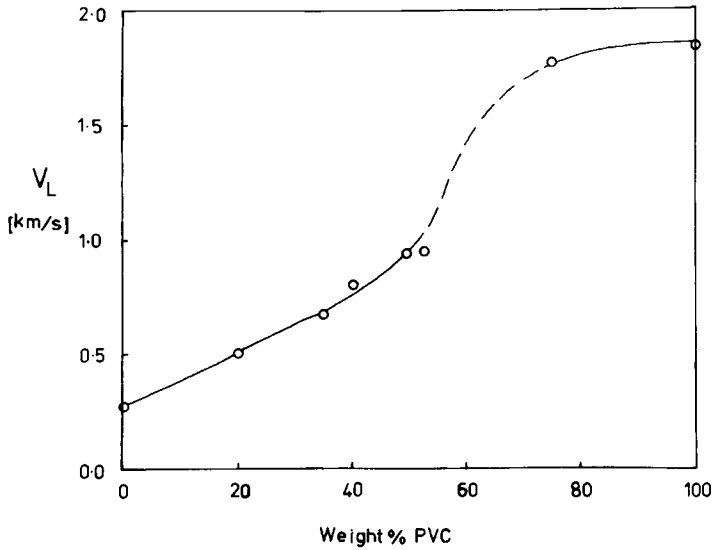


Fig. 3. Longitudinal sonic velocity (V_L) vs weight percent PVC for the homopolymers and the blends.

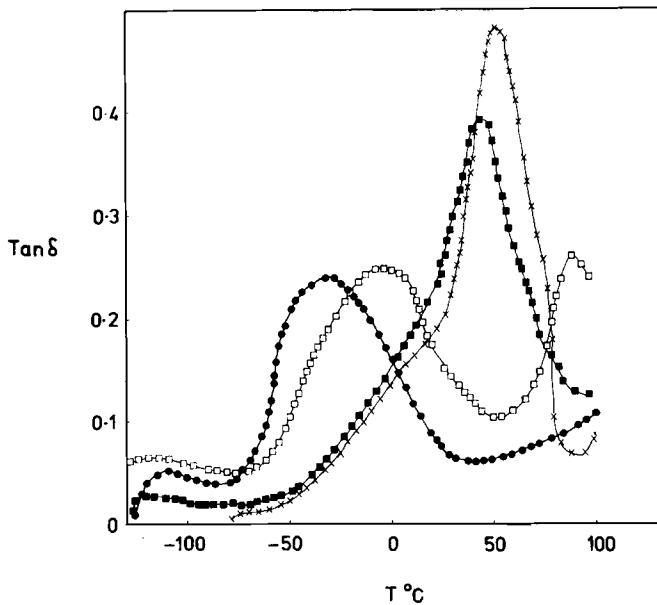


Fig. 4. Plots of $\tan \delta$ vs temperature for Hytrel (●) and blends containing 80% (□), 65% (■), and 60% (X) Hytrel. The frequency was 110 Hz.

peaks in the $\tan \delta$ -temperature dispersion (Fig. 4), indicating the presence of both a soft segment/PVC phase and a largely pure PVC phase which at this level of composition will be discontinuous. Nevertheless, this sample lies on the same line (Fig. 3) as the other compatible blends. As this technique utilizes sonic pulses having a wavelength of around 2 cm, it is only sensitive to the blend composition and to the nature of the continuous phase.

The acoustic impedance shows the same trends as V_L when plotted against

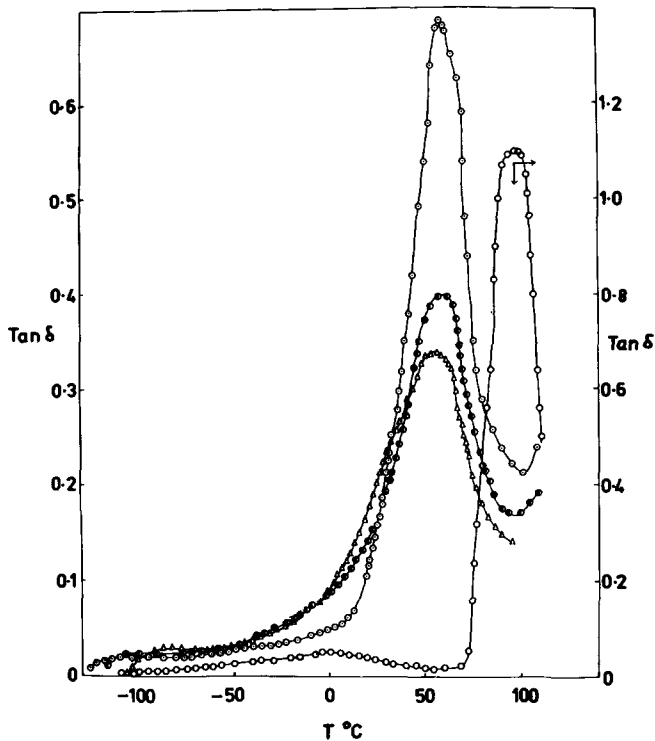


Fig. 5. Plots of $\tan \delta$ vs temperature for PVC (O) and blends containing 50% (Δ), 45% (\bullet), and 25% (\circ) Hytrel. The frequency was 110 Hz.

weight percent PVC. The acoustic impedance of PVC is very similar to that of polystyrene, which has a reported¹⁸ value of $0.25 \times 10^6 \text{ g cm}^{-2} \text{ s}^{-1}$.

Figures 4 and 5 show the Rheovibron $\tan \delta$ -temperature curves for both homopolymers and for all six blends. All the blends, except the one with 80% Hytrel, show a single glass transition, indicating, at least, a very high level of compatibility.

The Hytrel sample showed two peaks, one at -111°C and the other at -32°C . As it has been shown¹³ that the magnitude of the lower temperature transition is dependent on the weight fraction of soft segments, it could be the result of a

TABLE III
Certain Dynamic Mechanical Properties of the Homopolymers and Blends (110 Hz)

Composition ^a	T_g , $^\circ\text{C}$	$\tan \delta_{\max}$ ^b	ΔH , kcal/mole ^c
100	-32	0.24	27.5 (~15)
80	-5, 87	0.25, 0.26	—
65	44	0.40	75
60	49	0.48	55
50	59	0.34	—
45	62	0.40	—
25	63	0.69	125
0	97	1.10	67

^a Weight percent Hytrel in blends.

^b Maximum value of $\tan \delta$ in the glass transition region.

^c Apparent activation energy.

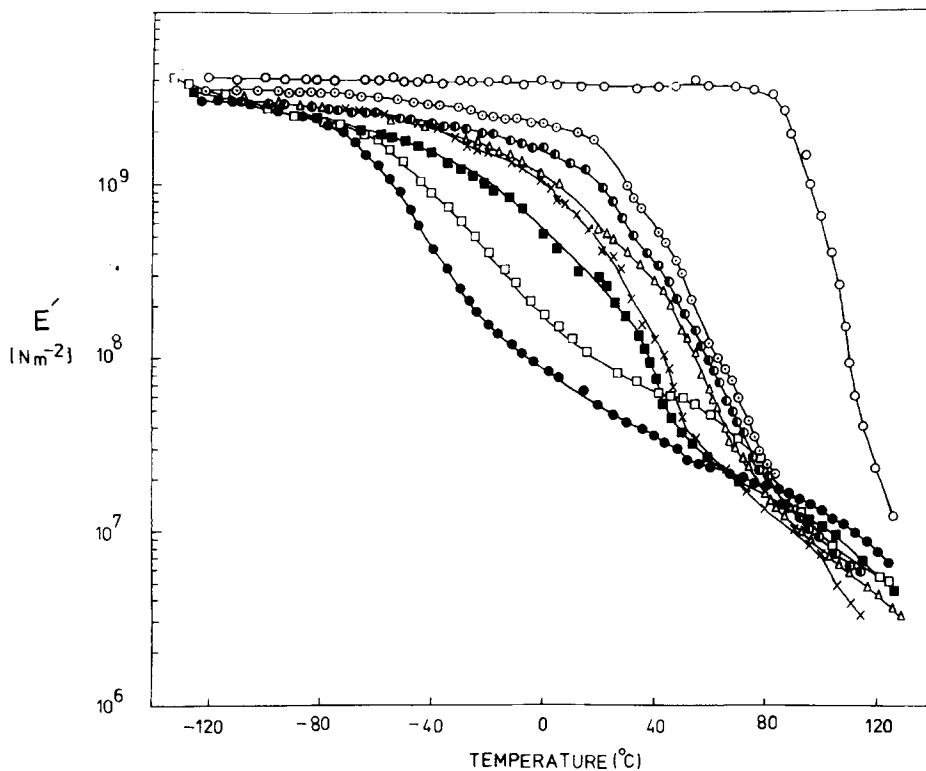


Fig. 6. Plots of dynamic storage modulus (E') vs temperature of PVC (○), Hytrel (●), and blends containing 80% (□), 65% (■), 60% (X), 50% (△), 45% (●), and 25% (○) Hytrel. The frequency was 110 Hz.

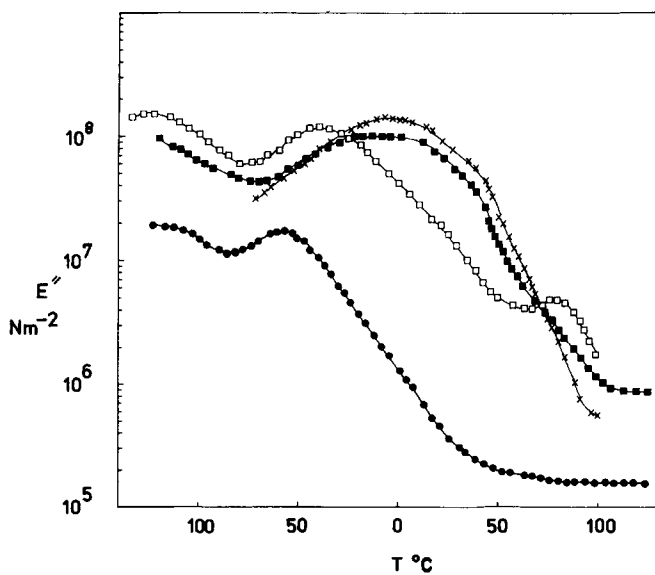


Fig. 7. Plots of dynamic loss modulus (E'') vs temperature for Hytrel (●) and blends containing 80% (□), 65% (■), and 60% (X) Hytrel. The frequency was 110 Hz.

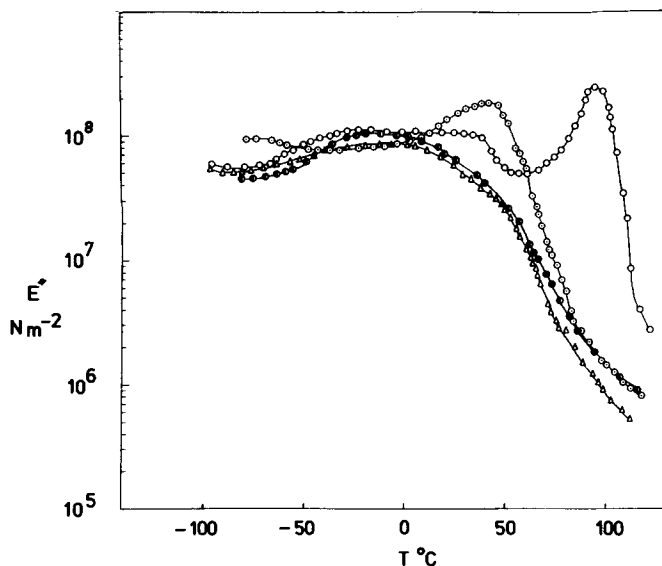


Fig. 8. Plots of dynamic loss modulus (E'') vs temperature for PVC (○) and blends containing 50% (△), 45% (●), and 25% (⊙) Hytrel. The frequency was 110 Hz.

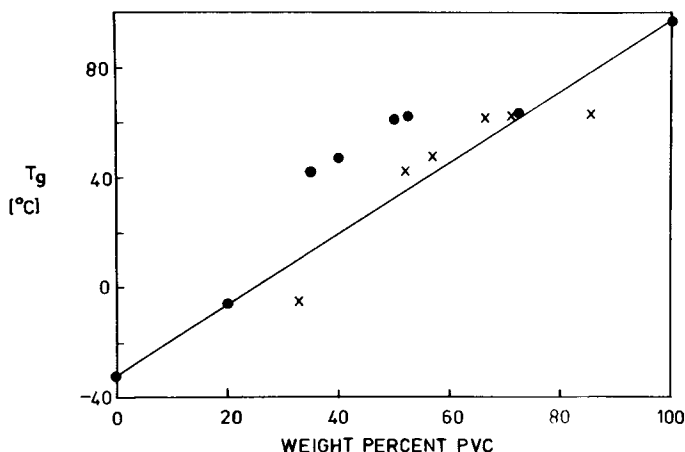


Fig. 9. Glass transition temperatures of the homopolymers and blends (T_g) vs weight percent PVC (●). The symbol (X) refers to the case where only the Hytrel soft segments are considered.

Schatzki-type mechanism involving the $(\text{CH}_2)_4\text{O}$ — soft-segment group. However, Wetton, and Williams¹⁹ have proposed that the mechanism for this low-temperature relaxation is a damped oscillation of the soft segments about their equilibrium positions. The transition at -32°C is the glass transition of the amorphous soft-segment phase.¹³ The PVC homopolymer also showed two transitions. There is a broad minor transition centered at -1°C and the glass transition at 97°C . These PVC transitions have been discussed by Pezzin et al.²⁰

Table III shows that the single glass transitions of all the blends, except the 80% Hytrel blend, moves progressively to lower temperatures with increasing Hytrel content. $\text{Tan } \delta_{\text{max}}$ decreases regularly from a value of 1.10 for PVC to 0.34

for the 50:50 blend. There is then an increase in $\tan \delta_{\max}$ for the blend containing 60% Hytrel. Both this blend and the one containing 65% Hytrel show shoulders on the low-temperature side of the curves suggesting the onset of phase separation. This is thought to be the reason for the increase in $\tan \delta_{\max}$.

Nishi et al.¹⁴ have reported a very broad transition for a 75% Hytrel/PVC blend and speculate that the two-component transitions are about to be resolved. This is verified in the case of our 80% Hytrel blend (Fig. 4) where there are two distinct loss peaks. They¹⁴ also comment on the fact that the low-temperature PVC transition moves to lower temperatures and decreases in size as the Hytrel level is increased. In this work, this minor transition certainly decreased rapidly with increasing copolyester content, but even at low Hytrel levels it soon became impossible to detect.

Figures 6, 7, and 8 show dynamic storage moduli (E')- and dynamic loss moduli (E'')-versus-temperature plots for all samples. The E' -temperature curves are typical of compatible blends in that only one transition region is discernible, except, of course, in the case of the 80% Hytrel blend where, again, two transition regions occur. This figure also shows the rather high elastic modulus of Hytrel, which is a particularly attractive feature of this rubbery polymer. The E'' -against-temperature curves (Figs. 7 and 8) show broad loss peaks for the fully compatible blends.

Table III also shows apparent activation energies for the homopolymer transitions and for those of three of the blends. The activation energies of the Hytrel and PVC glass transitions were 27.5 and 67 kcal/mole, respectively, while that for the low-temperature Hytrel transition was approximately 15 kcal/mole. For the 25% Hytrel blend, the activation energy was 125 kcal/mole, while for the 60% Hytrel blend, the value had dropped to 55 kcal/mole. The onset of incompatibility as shown by the shoulder on the $\tan \delta$ -temperature peak of the 65% Hytrel blend led to an increased value of 75 kcal/mole for this blend.

Figure 9 shows a plot of the glass transition temperature (T_g) determined from the position of $\tan \delta_{\max}$ (110 Hz) versus weight percent PVC. It is clear that there is not a simple linear relation between T_g of all the blends and their compositions. However, only the Hytrel soft segments are thought to be miscible with the PVC as the hard segments form separate crystalline domains. It is reasonable, therefore, only to consider the effect of mixing the Hytrel soft segments with the PVC. This latter plot shows that the glass transitions of compatible blends of PVC and Hytrel can be predicted to a good approximation by eq. (1):

$$T_{g\text{blend}} = W_1 T_{g_1} + W_2 T_{g_2} \quad (1)$$

where W_1 and W_2 are the weight fractions and T_{g_1} and T_{g_2} are the glass transition temperatures of the respective components of the blends. This conclusion is in agreement with the findings of Nishi et al.¹⁴

One of the authors (I.D.H.) wishes to thank the Science Research Council for a Research Studentship.

References

1. W. A. Utley, *Composites*, **6**, 34 (1974).
2. G. L. Ball and I. Salyer, *J. Acoust. Soc. Am.*, **39**, 663 (1966).
3. E. E. Ungar, in *Noise and Vibration Control*, L. L. Beranek, Ed., McGraw-Hill, New York, 1971, Chap. 14.

4. D. J. Williams, *Polymer Science and Engineering*, Prentice-Hall, Englewood Cliffs, N.J., 1971.
5. J. H. Aklonis, W. J. MacKnight, and M. Shen, *Introduction to Polymer Viscoelasticity*, Wiley-Interscience, New York, 1972.
6. H. Mizumachi, *J. Adhesion Soc. Jpn*, **5**, 370 (1969).
7. M. Matsuo, *Jpn Plast.*, **2**, 6 (1968).
8. L. H. Sperling, Tai-Woo Chiu, R. G. Gramlich, and D. A. Thomas, *J. Paint Technol.*, **46**, 47 (1974).
9. J. A. Grates, D. A. Thomas, E. C. Hickey, and L. H. Sperling, *J. Appl. Polym. Sci.*, **19**, 1731 (1975).
10. R. J. Cella, *J. Polym. Sci.*, **C42**, 727 (1973).
11. R. W. Seymour, J. R. Overton, and L. S. Corley, *Macromolecules*, **8**, 331 (1975).
12. M. Brown, *Rubber Ind.*, **9**, 102 (1975).
13. M. Shen, V. Mehra, N. Niinomi, J. T. Koberstein, and S. L. Cooper, *J. Appl. Phys.*, **45**, 4182 (1974).
14. T. Nishi, T. K. Kwei, and T. T. Wang, *J. Appl. Phys.*, **46**, 4157 (1975).
15. T. Nishi and T. K. Kwei, *J. Appl. Polym. Sci.*, **20**, 1331 (1976).
16. *Encyclopaedia of Polymer Science and Technology*, Vol. 11, p. 69.
17. *Encyclopaedia of Polymer Science and Technology*, Vol. 11, p. 71.
18. R. W. B. Stephens, in *Physics of Plastics*, P. D. Ritchie, Ed., Iliffe Books, London, 1965, Chap. 9.
19. R. Wetton and G. Williams, *Trans. Faraday Soc.*, **61**, 2132 (1965).
20. G. Pezzin, G. Ajroldi, T. Casiraghi, C. Garbuglio, and G. Vittadini, *J. Appl. Polym. Sci.*, **16**, 1839 (1972).

Received August 2, 1976

Revised October 26, 1976